



Significance of the Lesion–Pleura Relationship in Differentiating Peripheral Inflammatory Lesions and Lung Cancers

Yang Tao*, Wen-Tao Zhang*, Can Ding, Bin-Jie Fu , Fa-Jin Lv, Zhi-Gang Chu 

Department of Radiology, The First Affiliated Hospital of Chongqing Medical University, Chongqing, People's Republic of China

*These authors contributed equally to this work

Correspondence: Fa-Jin Lv; Zhi-Gang Chu, Department of Radiology, The First Affiliated Hospital of Chongqing Medical University, 1# Youyi Road, Yuanjiagang, Yuzhong District, Chongqing, People's Republic of China, 400016, Tel +86 18723032809, Fax +86 23 68811487, Email cyscitg@hospital.cqmu.edu.cn; chuzg0815@163.com

Purpose: To determine the significance of lesion–pleura relationship in differentiating peripheral inflammatory lesions (PILs) and peripheral lung cancers (PLCs).

Patients and Methods: From January 2017 to April 2022, a total of 743 patients with 501 PLCs and 292 PILs (≥ 1.5 cm) were retrospectively enrolled. The patients' clinical characteristics and CT features of lesions in these two groups were analyzed and compared, and the impact of the lesion–pleura relationship (broad or narrow basement and distance between lesion and pleura) on differentiation was specifically assessed.

Results: Lesions attached to pleura were more frequent in PILs (188, 64.4%) than in PLCs (244, 48.7%) ($P < 0.001$), and those with broad basement-to-pleura were also more common in PILs (133, 70.7%) than in PLCs (47, 19.3%) ($P < 0.001$). Among the 296 lesions with a lesion-pleura distance ≤ 16 mm, the optimal cutoff value of distance was ≤ 8.9 mm (area under curve [AUC], 0.733; sensitivity: 0.770; specificity: 0.623; $P < 0.001$) for predicting PLCs. Regarding the 728 lesions attached to pleura or with a lesion-pleura distance ≤ 16 mm, the AUC of the model based on the clinical and CT features for predicting PLCs significantly increased from 0.812 to 0.879 after including lesion-pleura relationship (narrow basement or lesion-pleura distance ≤ 8.9 mm) ($P < 0.001$). Additionally, the lesion–pleura relationship was one of independent indicators for differentiation (odds ratio, 9.433; $P < 0.001$).

Conclusion: When differentiating peripheral lesions (≥ 1.5 cm), it is crucial to consider the basement-to-pleura and lesion-pleura distance besides patients' clinical characteristics, laboratory parameters and morphological features.

Keywords: lung neoplasms, diagnosis, differential, tomography, X-ray computed

Introduction

Lung cancer remains the most prevalent and deadliest cancer worldwide.¹ On computed tomography (CT) images, lung cancer typically appears as either a central or peripheral lesion, with peripheral lung cancers (PLCs) denoting lesions situated in the outer regions of the lung. PLCs often manifest as subpleural nodules or masses, a presentation also observed in peripheral inflammatory lesions (PILs).^{2,3} The similarity in location and morphological features between PLCs and PILs poses a significant diagnostic challenge, potentially leading to delayed cancer treatment or unnecessary surgical procedures for inflammatory conditions.^{4,5} Therefore, accurate differentiation between these two conditions is necessary.

The nature of peripheral nodules or masses could be determined by analyzing their characteristics observed on CT scans.⁶ Various CT features have been consistently assessed to differentiate malignant and benign lesions.^{7–9} Specifically, most of lesions manifested as ground-glass opacity can be differentiated by a detailed assessment of CT features and their changes in long-term follow-up.^{10,11} However, the CT features of solid lesions usually overlap, and long-term follow-up

carries some risk. Though common CT features, such as lobulation and spiculation sign, vascular convergence sign, and well-defined boundary, are highly suggestive of lung cancer,^{8,12} these indicators are not specific and misdiagnoses still occur, highlighting the need for additional predictors.

Considering that peripheral lesions are in close proximity to the pleura, the relationship between them may provide additional diagnostic information in differentiation.¹³ Previous studies have primarily focused on evaluating pleural invasion, as it is a crucial factor in grading PLCs and determining appropriate surgical strategies.^{14,15} However, despite these findings, the detailed lesion-pleura relationship, such as the basement-to-pleura and lesion-pleura distance, has not been extensively investigated in the context of their differential diagnosis. Further research into this aspect may potentially enhance the accuracy of distinguishing between PLCs and PILs.

The lesion-pleura relationship can be classified into two main conditions: lesions that are either attached to the pleura or distanced from it. Attached lesions may exhibit either a broad or narrow basement, while distanced lesions may display varying spatial distance between pleura. Based on this observation, we hypothesize that the lesion-pleura relationship could provide important diagnostic clues. Therefore, the aim of this study is to determine the potential diagnostic significance of the relationship between pulmonary lesions and the pleura.

Materials and Methods

Patients

This single-center retrospective study was approved by the institutional review board of the First Affiliated Hospital of Chongqing Medical University, and the requirement for informed consent from the patients was waived due to the retrospective nature of this study.

Patients with confirmed pulmonary solid nodules or masses were retrospectively enrolled in this study based on the electronic health record (EHR) and picture archiving and communications system (PACS). Firstly, the EHR was reviewed to identify all patients who underwent treatment of pulmonary lesions in the department of thoracic surgery and respiratory from January 2017 to April 2022. The search results were reviewed to identify cases with pathologically confirmed pulmonary lesions and those with inflammatory lesions confirmed by follow-up after anti-inflammatory treatment. Secondly, cases were manually reviewed by a fellowship-trained thoracic radiologist with 3 years of experience in chest imaging to confirm whether they had chest CT images in the PACS, lesions were central type or peripheral type, and lesions were nodules, masses, or others. Patients without chest CT data, those with central-type lesions, and cases where lesions were not presented as nodules or masses were excluded. This is because PILs and PLCs that manifest as nodules or masses typically share similar morphological features, making them difficult to differentiate clearly on CT images. Thirdly, cases were reviewed by a senior thoracic radiologist with 8 years of experience in chest imaging to determine lesion diameter and attenuation (solid or part-solid) on CT images. The lesions ≤ 15 mm in diameter or manifested as part-solid nodules (PSNs) were excluded, because solid nodules >15 mm in diameter or masses are regarded with high suspicion of cancers according to Lung-RADS criteria,¹⁶ and benign and malignant PSNs usually had distinct CT features. After preliminarily selecting, the residual patients with solid lung cancers ($n = 498$) and benign lesions ($n = 381$) were candidates for this study. From these 879 patients, those had only thick-section CT images with a thickness greater than 1 mm ($n = 27$) (as accurate evaluation of the distance between lesion and pleura was not feasible on thick-slice images), lesions attached to the interlobular fissure ($n = 24$) (as the differences between interlobular pleura and pleura adjacent to mediastinum and chest wall may affect the lesion-pleura relationship) or tuberculomas and benign tumors ($n = 68$) (as they usually exhibit typical features distinct from those of inflammatory lesions), and artifacts or noise on CT images compromising accurate evaluation ($n = 17$), were excluded. Finally, 463 patients with 501 PLCs and 280 patients with 292 PILs were included in this study.

CT Examinations

All CT images were obtained using one of the following CT scanners: SOMATOM Perspective (Siemens Healthineers, Erlangen, Germany), SOMATOM Definition Flash (Siemens Healthineers, Erlangen, Germany), or Discovery CT750 HD (GE Healthcare, Milwaukee, WI, USA). All CT scans were performed with the patient in a supine position from the

thoracic entrance to the costophrenic angle at the end of inspiration during a single breath-hold. A breath-hold exercise was implemented before each examination. The following were the scan parameters: tube voltage, 120 kVp; tube current time, 50–140 mA (using automatic current modulation technology); scanning slice thickness, 5 mm; rotation time, 0.5 s; pitch, 1–1.1; collimation, 0.6 or 0.625 mm; reconstruction slice thickness and interval, 0.625 or 1 mm; matrix, 512×512. All patients underwent plain CT scan, 451 patients (56.9%), comprising 99 with PILs and 352 with PLCs, also underwent contrast-enhanced CT scan with a total of 80–100 mL of nonionic iodinated contrast material (Iopamidol, 320 mg/mL; Shanghai Bracco Sine Pharmaceutical Co., Ltd., China) at an injection rate of 3.0 mL/s, followed by 50 mL of saline solution via a power injector.

Image Analysis

Two radiologists with 15 and 8 years of experience in chest imaging who were blinded to the pathological results and clinical data independently evaluated the CT images. The CT data were analyzed in both the lung window setting (level, –600 hU; width, 1200 hU) and the mediastinal window (level, 40 hU; width, 400 hU) by using Carestream Vue PACS (Carestream, Rochester, NY, USA). Any discrepancy between the two radiologists was resolved by reevaluating the images together and repeatedly measuring the parameters on same section with same window level and width.

The following CT features of pulmonary lesions were analyzed based on the plain CT images because not all the patients had enhanced CT data: size (the mean of the longest diameter and the perpendicular diameter on axial CT images), location (upper, middle and lower lobe), shape (regular [round and oval] or irregular), lobulation, spiculation, boundary (well-defined or ill-defined), R-length, adjacent pleural thickening, and the distance between lesions and pleura. Lobulation was defined as an abrupt bulging of the contour of the lesion.¹⁷ Spiculation sign was defined as linear strands that extended from the nodule surface into the lung parenchyma without reaching a pleural surface.¹⁷ R-length was used for describing the tightness between lesion and pleura, which was calculated by dividing the length of the longest part where the lesion touched the pleura on transverse, coronal, or sagittal CT images by the widest part of the lesion that was parallel to the pleura. R-length ≥ 1 indicated broad basement, or it was narrow basement (Figure 1). Pleural thickening was defined as a visible increase in pleural thickness beyond the normal pleural appearance.¹⁸ Following the methodology of Ebara and colleagues,¹⁹ we measured the lesion-to-pleura distances obtained from transverse, coronal, and sagittal CT images, and specifically recorded the minimum distance (referred to as D-length) (Figure 1).

Statistical Analysis

Statistical analyses were conducted using SPSS (version 25.0, IBM, NY, USA). Continuous data were presented as mean \pm standard deviation, and categorical data as counts and percentages. Mann–Whitney *U*-test was used for continuous data and Pearson chi-square was used for categorical data. Receiver operating characteristic (ROC) curves were constructed to evaluate the diagnostic accuracy of the D-lengths, and the area under curve (AUC) was utilized to evaluate the predictive effectiveness. The max Youden index of ROCs with highest AUC was then calculated to identify the diagnostic cutoff point. Logistic regression analysis was performed to construct models for predicting PLCs. DeLong test was used to compare the AUCs of the models based on clinical, CT features and relationship between lesions and pleura. A *P*-value below 0.05 was considered statistically significant.

Results

Patient' Clinical Characteristics and CT Features of Lesions

Among the 292 PILs, 241 (82.5%) were confirmed as nonspecific inflammatory lesions, 12 (4.1%) as fungal infections, and 30 (10.3%) as viral infections, and 9 (3.1%) were completely absorbed during follow-up after anti-inflammatory treatment. The 501 PLCs consisted of 395 (78.8%) adenocarcinomas, 74 (14.8%) squamous cell carcinomas, 23 (4.6%) adenosquamous carcinomas, and 9 (1.8%) small cell lung cancers. The patients' clinical characteristics and CT features of lesions are listed in Table 1. Compared with PLCs, the PILs were smaller and cases with spiculation and lobulation sign in them were less common (each *P* < 0.05).

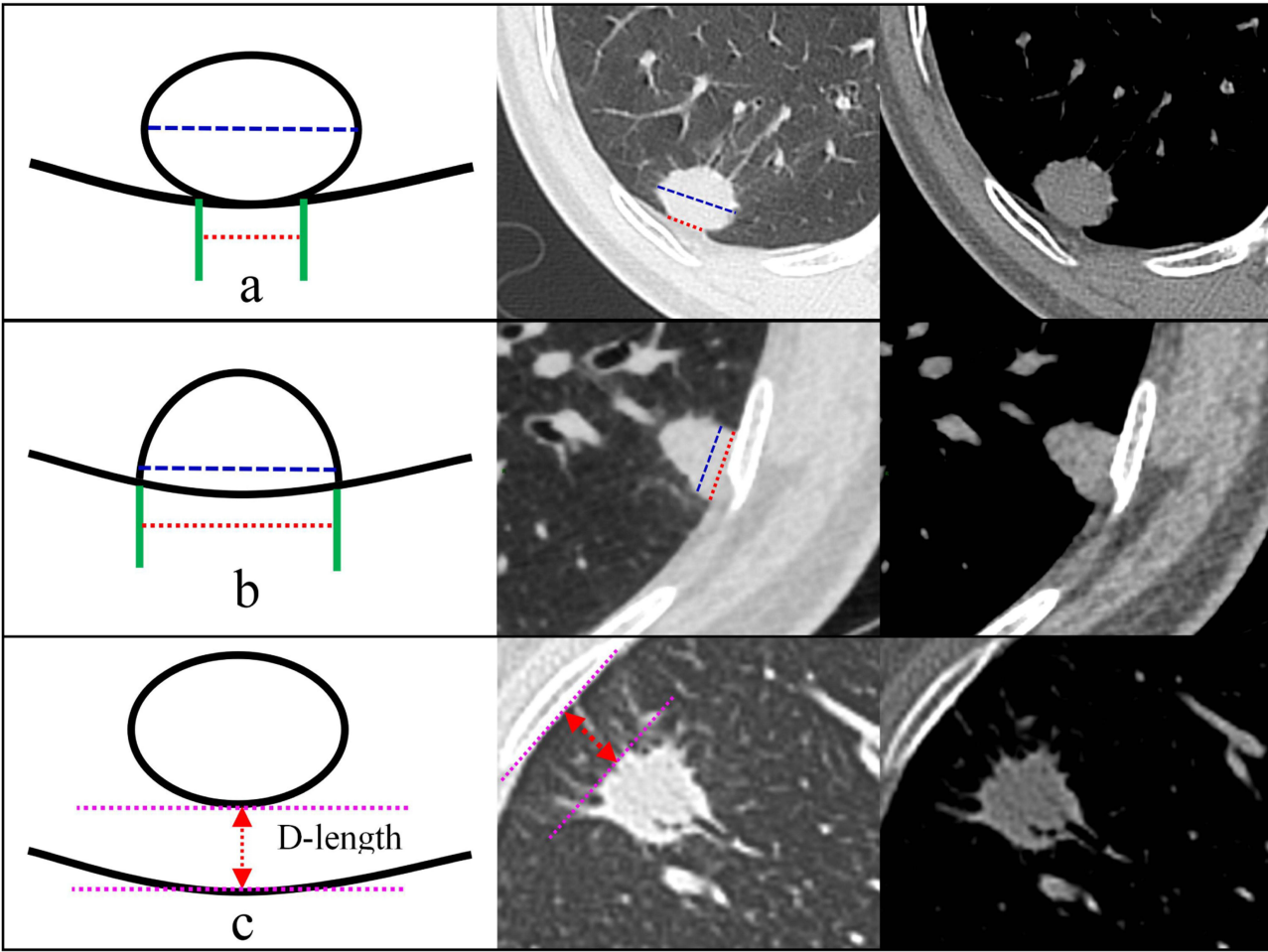


Figure 1 Relationship between lesions and pleura on CT images. For the lesions attached to pleura, R-length is defined as the ratio of the length of the greatest lesion–pleura interface (red-dashed line) to maximum diameter (blue-dashed line) of the lesion parallel to the pleura. R-length < 1 indicates narrow basement (**a**), the corresponding CT images at right side show a nodule attached to pleura with narrow basement (the length of red dashed line [10.4 mm] is significantly shorter than that of blue dashed line [23.2 mm]). R-length ≥ 1 indicates broad basement (**b**), the corresponding CT images at right side show a nodule attached to pleura with broad basement (the length of red dashed line [16.5 mm] is slightly greater to that of blue dashed line [15.8 mm]). For the lesions not attached to pleura, the distance between lesion and pleura (D-length) is measured (**c**). The corresponding CT images at right side show a nodule not attached to pleura, and the vertical distance between the distal edge of nodule and pleura (arrows) is 12.1 mm.

Relationship Between Lesions and Pleura

Among the 793 lesions, 432 (54.5%) were identified to be attached to the pleura. The numbers of cases attached to pleura in the PILs and PLCs were 188 (64.4%) and 244 (48.7%), respectively. The lesions attached to pleura were more

Table 1 The Patients’ Clinical Characteristics and CT Features of Lesions

| Indicators | PLCs (n = 501) | PILs (n = 292) | P-value |
|-----------------|----------------|----------------|---------|
| Gender* | | | 0.456 |
| Male | 264 (57.0) | 151 (53.9) | |
| Female | 199 (43.0) | 129 (46.1) | |
| Age (years) | 58.24 ± 9.4 | 55.97 ± 10.6 | 0.089 |
| Smoking history | | | 0.010 |
| Yes | 270 (58.3) | 128 (45.7) | |
| No | 193 (41.7) | 152 (54.3) | |

(Continued)

Table 1 (Continued).

| Indicators | PLCs (n = 501) | PILs (n = 292) | P-value |
|----------------------|----------------|----------------|---------|
| Diameter (mm) | 23.7 ± 7.4 | 22 ± 7.0 | 0.001 |
| Location | | | 0.118 |
| Upper lobe | 272 (54.3) | 176 (60.3) | |
| Middle or lower lobe | 229 (45.7) | 116 (39.7) | |
| Shape | | | 0.082 |
| Irregular | 267 (53.3) | 175 (59.9) | |
| Regular | 234 (46.7) | 117 (40.1) | |
| Spiculation | | | < 0.001 |
| Yes | 215 (42.9) | 59 (20.2) | |
| No | 286 (57.1) | 233 (79.8) | |
| Lobulation | | | < 0.001 |
| Yes | 342 (68.3) | 75 (25.7) | |
| No | 159 (31.7) | 217 (74.3) | |
| Boundary | | | < 0.001 |
| Well-defined | 441 (88.0) | 208 (71.2) | |
| Ill-defined | 60 (12.0) | 84 (28.8) | |
| Pleural thickening | | | 0.117 |
| Yes | 101 (20.2) | 45 (15.4) | |
| No | 400 (79.8) | 247 (84.6) | |

Notes: Data are expressed as number (percentage) or mean ± standard deviation. *There were 463 patients with 501 PLCs, and 280 patients with 292 PILs.

common in the PILs than in PLCs ($P < 0.001$). Among the lesions attached to pleura, number of cases with broad and narrow basement in the PILs and PLCs were 133 (70.7%) and 55 (29.3%), and 47 (19.3%) and 197 (80.7%), respectively. Compared with PLCs, lesions with broad basement were more common in PILs (70.7% vs 19.3%, $P < 0.001$).

Among the 361 lesions with distance between lesions and pleura, 257 (71.2%) were PLCs and 104 (28.8%) were PILs. The D-lengths of PLCs (mean: 8.3 ± 6.4 mm, range: 0.5 to 29.9 mm) were greater than those of PILs (mean: 13.1 ± 7.3 mm, range: 2.8 to 37.9 mm) ($P < 0.001$). Based on the D-lengths of total lesions (range: 0.5 to 37.9 mm), these lesions were categorized into 38 groups with 1 mm interval based the D-length (eg, group 1: D-length ≤ 1 mm, group 2: D-length ≤ 2 mm, group 38: D-length ≤ 38 mm). Within group 16, the proportions of lesions in PLC group were all significantly higher than those in PIL group (each $P < 0.05$), which indicated that the D-length was more effective for differentiating them among the lesions with a D-length ≤ 16 mm. Among the 296 lesions with a D-length ≤ 16 mm, the optimal cutoff value for distinguishing PLCs from PILs obtained by using ROC analysis was ≤ 8.9 mm (AUC, 0.733; sensitivity: 0.770; specificity: 0.623; $P < 0.001$).

Logistic Regression Model

The regression models were constructed based on the clinical and CT features of lesions with statistical differences. Positive relationship between lesion and pleura was defined as a narrow basement-to-pleura or a shorter D-length (≤ 8.9 mm). Models A and B for predicting PLCs were performed based on the patients' clinical characteristics and CT features of lesions, and a combination of patients' clinical characteristics, CT features of lesions, and the relationship between lesion and pleura, respectively. Among the 793 lesions, 65 including 39 PLCs and 26 PILs with a D-length of > 16 mm were not studied in these models because the D-length was not an indicator for distinguishing them. For the residual 728 lesions, there were significant differences in AUC between model A (AUC: 0.812, 95% CI: 0.773–0.832; sensitivity: 71.21%, specificity: 78.20%; positive predictive value [PPV]: 85.01%, negative predictive value [NPV]: 61.00%) and model B (AUC: 0.879, 95% CI: 0.853–0.902; sensitivity: 78.35%, specificity: 84.21%; PPV: 89.60%, NPV: 69.13%) (Figure 2). Moreover, model B revealed that smoking history (Odds ratio [OR], 2.194; 95% CI, 1.435–3.354; $P < 0.001$), diameter ≥ 18.9 mm (OR, 1.004; 95% CI, 1.001–1.007; $P < 0.0001$), spiculation (OR, 2.590; 95% CI,

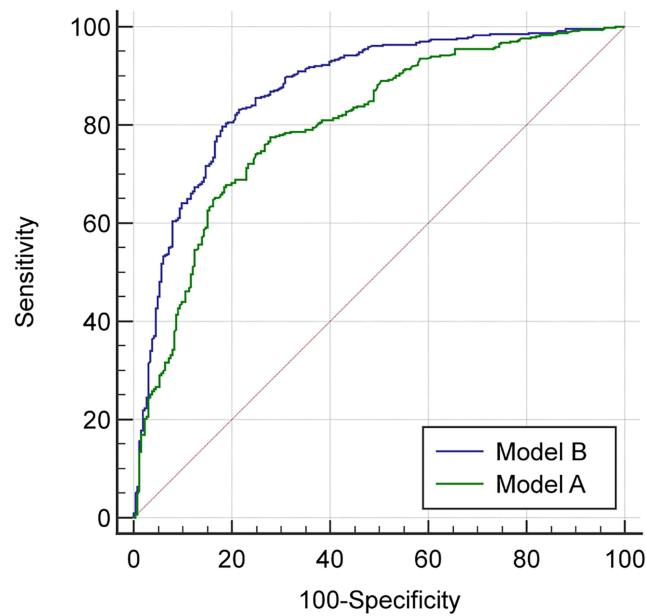


Figure 2 ROC curves of model A and model B. After incorporating the relationship between lesions and pleura, the performance of model A was significantly improved (AUC of model (A) 0.812, AUC of model (B) 0.879).
Abbreviation: ROC, receiver operating characteristic; AUC, area under curve.

1.648–4.069; $P < 0.001$), lobulation (OR, 7.439; 95% CI, 4.851–11.407; $P < 0.001$), well-defined boundary (OR, 3.708; 95% CI, 2.446–5.622; $P < 0.001$), and positive relationship between lesion and pleura (OR, 9.433; 95% CI, 6.191–14.374; $P < 0.0001$) were independent indicators for predicting PLCs (Table 2) (Figure 3).

Table 2 Multivariate Logistic Regression for Predicting PLCs

| Variables | Odds Ratio (95% CI) | P-value |
|--------------------------|----------------------|---------|
| Smoking history | | < 0.001 |
| Yes | 2.194 (1.435–3.354) | |
| No | 1 | |
| Diameter (mm) | | 0.008 |
| ≥ 18.98 | 1.004 (1.001–1.007) | |
| < 18.98 | 1 | |
| Spiculation | | < 0.001 |
| Yes | 2.590 (1.648–4.069) | |
| No | 1 | |
| Lobulation | | < 0.001 |
| Yes | 7.439 (4.851–11.407) | |
| No | 1 | |
| Boundary | | < 0.001 |
| Well-defined | 3.708 (2.446–5.622) | |
| Ill-defined | 1 | |
| Pleural thickening | | 0.017 |
| Yes | 0.430 (0.240–0.772) | |
| No | 1 | |
| Relationship with pleura | | < 0.001 |
| Positive | 9.433 (6.191–14.374) | |
| Negative | 1 | |

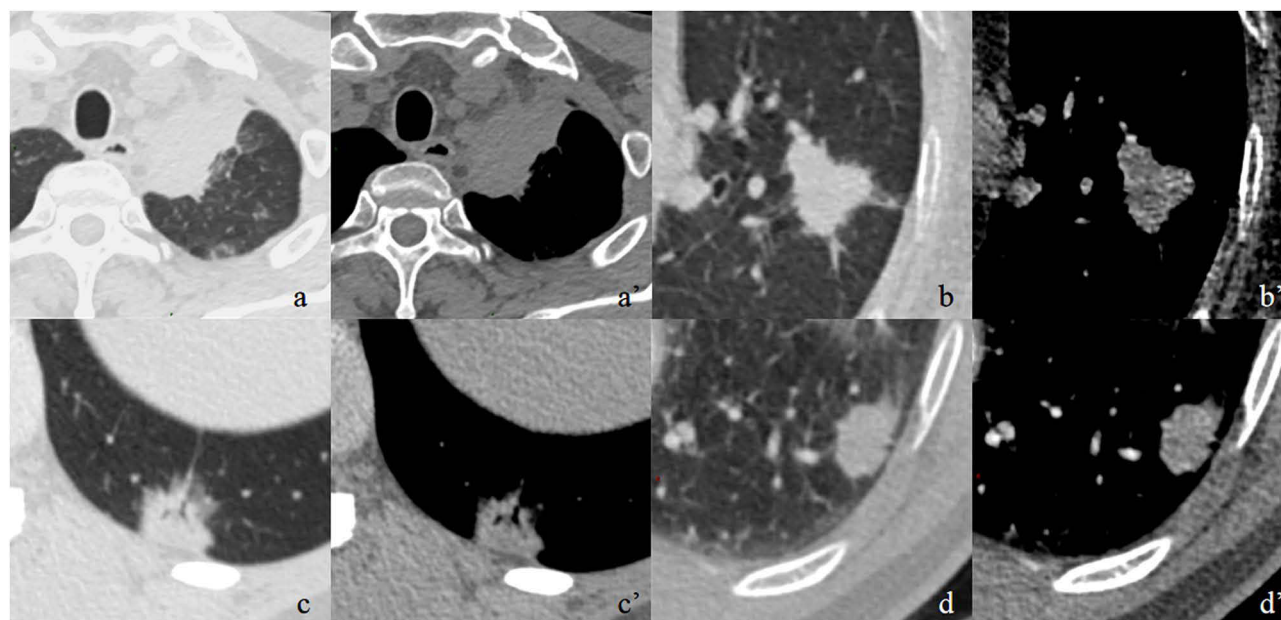


Figure 3 A 54-year-old male has a solid, well-defined, and slightly lobulated mass (36.5 mm in diameter) located in the left upper lobe with a broad basement to mediastinal pleura, which is pathologically confirmed as an inflammatory lesion after operation (a, a'). A 48-year-old female has a solid, well-defined, lobulated, and spiculated nodule (19.5 mm in diameter) located in the left upper lobe with a greater distance to pleura (10.9 mm), which is pathologically confirmed as fungal infection after operation (b, b'). A 35-year-old female has a spiculated and well-defined solid nodule (15.6 mm in diameter) with air-bronchogram located in the left lower lobe with a narrow basement to pleura, which is pathologically confirmed as invasive adenocarcinoma after operation (c, c'). A 75-year-old male has a solid and well-defined nodule (18.7 mm in diameter) located in the left lower lobe with a shorter distance to pleura (0.9 mm), which is pathologically confirmed as invasive adenocarcinoma after operation (d, d').

Discussion

Pulmonary peripheral lesions, which mainly include PLCs and PILs, often present similar CT manifestations, leading to frequent misdiagnoses.²⁰ Despite their proximity to the pleura, the relationship between lesion and pleura has not been thoroughly explored, and its diagnostic value in differentiation remains unclear. This study investigated the contact pattern of lesions attached to pleura and the distance of lesions not in contact with the pleura to determine their differentiation potential. The findings revealed that PLCs typically exhibit smaller lesion-pleura gaps or a narrow basement to pleura, whereas PILs tend to have greater lesion-pleura gaps or a broad basement to pleura. By considering the lesion-pleura relationships, the diagnostic efficiency of common clinical and CT features was significantly improved. Therefore, these results strongly suggest that the relationship between peripheral lesions and pleura should be taken into account when distinguishing them.

Previous studies have extensively investigated the role of morphological features in differentiating PLCs from PILs, indicating that characteristics such as ill-defined boundary, oval shape, hypodense sign, pleural thickening, and halo sign are more commonly observed in PILs.^{21–23} Moreover, when these features are insufficient for an accurate diagnosis, incorporating machine learning-based radiomics can enhance diagnostic precision.^{24,25} However, there remains uncertainty regarding which specific feature is most valuable for differential diagnosis. PLCs and PILs demonstrate distinct relationships with the pleura. Although it has been reported that a broad basement to pleura and embedding in thickened pleura are predominantly associated with PILs,²⁶ their spatial relationship has not been thoroughly investigated.

In this study, it was found that the PLCs frequently had a smaller distance to pleura or a narrow basement. In contrast, the PILs were generally observed to be either distantly located from the pleura or closely adhered to it with a wide basement. These characteristics may be related to the occurrence and development of lesions. Previous research has suggested that pulmonary inflammatory lesions often involve subpleural lung tissue.^{27,28} Furthermore, the abundant blood supply and lymphatic system beneath the pleura facilitate the rapid spread of inflammation, potentially leading to absence of narrow lesion-pleura gap but a broad attachment to the pleura.²⁹ However, lung cancers typically display a spherical shape that can be round or oval and develop gradually.^{27,30} Their outward expansion and infiltration is

relatively limited and slow. Thus, PLCs typically maintain a certain gap between lesions and the pleura. Even when they are in close contact with the pleura due to reaching a certain size, they mainly present with a narrow basement.

Though the lesion-pleura distance is a useful indicator for differentiating PILs and PLCs, its applicability is limited to cases with a measurable distance. In this study, only cases with a distance less than 16 mm could be effectively distinguished using this indicator. Within this range, a distance of ≤ 8.9 mm suggests a higher likelihood of lung cancer. This trend may be attributed to PLCs exhibiting a more continuous distance to the pleura than PILs, thus being more prevalent among lesions with a small distance. In contrast, the observation that being far away from the pleura is a common feature of both PLCs and PILs. Furthermore, PLCs and PILs may exhibit overlapping manifestations at different stages. Before extensively involving the lung tissue, PILs may have a narrower basement or a smaller distance to the pleura, while PLCs could also present with no distance or a broad basement once the lesion reaches a significant size. Therefore, when differentiating peripheral lesions, it is crucial to consider other CT features as a primary factor, such as the lobulation sign, with the characteristics of the lesion-pleura relationship serving as a significant supplement.

Through logistic regression analysis, it was determined that smoking history, large diameter, spiculation, lobulation, well-defined boundary, and a positive relationship with the pleura are all independent indicators of PLCs. Smoking is the primary risk factor for lung cancer.³¹ Lung cancers in smokers often grow more rapidly and typically present larger sizes with malignant features such as spiculation and lobulation at the time of diagnosis.³² As the tumor progresses, the tumor cells within the lesions become denser and thicker, without causing significant inflammation or exudation in adjacent tissues.³³ Consequently, these tumors are usually well defined, and consolidation of surrounding lung tissue or pleural thickening is rare. In contrast, they generally maintain a small distance from the pleura or exhibit a narrow basement-to-pleura.

This study had several limitations. First, it was retrospective and conducted at a single center, with the sample size of confirmed PILs being relatively small. Secondly, as this study solely assessed pulmonary lesions with a diameter ≥ 1.5 cm, the diagnostic significance of the lesion-pleura relationship for smaller solid lesions remains uncertain. Third, tuberculomas and benign tumors were not included in the study, as they often present distinct features on CT images. Fourth, patients with only thick-section CT scans were excluded, limiting the applicability of present findings to thin-section images. Fifth, the enhancement characteristics were not assessed for differentiation, as not all cases underwent enhanced CT scans. Lastly, since PLCs and PILs with a distance to the pleura >16 mm did not show significant differences in the lesion-pleura relationship, the findings should not be used to assess their likelihood. Instead, in clinical practice, these findings should be considered alongside other clinical and imaging features for accurate evaluation.

Conclusion

In addition to patients' clinical characteristics and morphological CT features of lesions, the relationship between pulmonary nodules or masses and pleura holds significant diagnostic value in differentiating common pulmonary peripheral lesions. Among peripheral lesions with a lesion-pleura distance ≤ 16 mm, smaller lesion-pleura gaps (≤ 8.9 mm) or a narrow basement to the pleura serve as indicators of PLCs, whereas PILs tend to exhibit greater lesion-pleura gaps (>8.9 mm) or a broad basement to the pleura. By incorporating these lesion-pleura relationships, the diagnostic accuracy of clinical and CT features is notably enhanced. Therefore, when distinguishing larger pulmonary peripheral solid nodules and masses (>1.5 cm), it is essential to consider the relationship between the lesions and the pleura.

Ethics Statement

The study was conducted in accordance with the Declaration of Helsinki, and the protocol was approved by the Ethics Committee of the First Affiliated Hospital of Chongqing Medical University (No. 2019-062), which absolved the need for written informed consent because of the retrospective study. All personal identification data were anonymized and de-identified before analysis.

Funding

This work was supported by the Project of Chongqing Natural Science Foundation (CSTB2024NSCQ-MSX0655) and the Senior Medical Talents Program of Chongqing for Young and Middle-aged from Chongqing Health Commission (Receptor: Zhi-gang Chu).

Disclosure

All authors declare no conflicts of interest for this work.

References

- de Martel C, Georges D, Bray F, Ferlay J, Clifford GM. Global burden of cancer attributable to infections in 2018: a worldwide incidence analysis. *Lancet Glob Health*. 2020;8(2):e180–e190. doi:10.1016/S2214-109X(19)30488-7
- Research T, Aberle DR, Adams AM, et al.; National Lung Screening Trial. Reduced lung-cancer mortality with low-dose computed tomographic screening. *N Engl J Med*. 2011;365(5):395–409. doi:10.1056/NEJMoa1102873
- Wahidi MM, Govert JA, Goudar RK, Gould MK, McCrory DC. American college of chest P. Evidence for the treatment of patients with pulmonary nodules: when is it lung cancer?: ACCP evidence-based clinical practice guidelines (2nd edition). *Chest*. 2007;132(3 Suppl):94S–107S. doi:10.1378/chest.07-1352
- Sobue T, Moriyama N, Kaneko M, et al. Screening for lung cancer with low-dose helical computed tomography: anti-lung cancer association project. *J Clin Oncol*. 2002;20(4):911–920. doi:10.1200/JCO.2002.20.4.911
- Sun Y, Li C, Jin L, et al. Radiomics for lung adenocarcinoma manifesting as pure ground-glass nodules: invasive prediction. *Eur Radiol*. 2020;30(7):3650–3659. doi:10.1007/s00330-020-06776-y
- Cai J, Vonder M, Heuvelmans MA, et al. CT characteristics of solid pulmonary nodules of never smokers versus smokers: a population-based study. *Eur J Radiol*. 2022;154:110410. doi:10.1016/j.ejrad.2022.110410
- Zhan Y, Peng X, Shan F, et al. Attenuation and morphologic characteristics distinguishing a ground-glass nodule measuring 5–10 mm in diameter as invasive lung adenocarcinoma on thin-slice CT. *AJR Am J Roentgenol*. 2019;213(4):W162–W170. doi:10.2214/AJR.18.21008
- Lin RY, Lv FJ, Fu BJ, Li WJ, Liang ZR, Chu ZG. Features for predicting absorbable pulmonary solid nodules as depicted on thin-section computed tomography. *J Inflamm Res*. 2021;14:2933–2939. doi:10.2147/JIR.S318125
- Mei X, Wang R, Yang W, et al. Predicting malignancy of pulmonary ground-glass nodules and their invasiveness by random forest. *J Thorac Dis*. 2018;10(1):458–463. doi:10.21037/jtd.2018.01.88
- Zhang Y, Shen Y, Qiang JW, Ye JD, Zhang J, Zhao RY. HRCT features distinguishing pre-invasive from invasive pulmonary adenocarcinomas appearing as ground-glass nodules. *Eur Radiol*. 2016;26(9):2921–2928. doi:10.1007/s00330-015-4131-3
- Liang J, Xu XQ, Xu H, et al. Using the CT features to differentiate invasive pulmonary adenocarcinoma from pre-invasive lesion appearing as pure or mixed ground-glass nodules. *Br J Radiol*. 2015;88(1053):20140811. doi:10.1259/bjr.20140811
- Zhou L, Zhou Z, Liu F, et al. Establishment and validation of a clinical model for diagnosing solitary pulmonary nodules. *J Surg Oncol*. 2022;126(7):1316–1329. doi:10.1002/jso.27041
- Zhao LL, Xie HK, Zhang LP, et al. Visceral pleural invasion in lung adenocarcinoma ≤ 3 cm with ground-glass opacity: a clinical, pathological and radiological study. *J Thorac Dis*. 2016;8(7):1788–1797. doi:10.21037/jtd.2016.05.90
- David E, Thall PF, Kalhor N, et al. Visceral pleural invasion is not predictive of survival in patients with lung cancer and smaller tumor size. *Ann Thorac Surg*. 2013;95(6):1872–1877. doi:10.1016/j.athoracsur.2013.03.085
- Wei SH, Zhang JM, Shi B, Gao F, Zhang ZX, Qian LT. The value of CT radiomics features to predict visceral pleural invasion in ≤ 3 cm peripheral type early non-small cell lung cancer. *J Xray Sci Technol*. 2022;30(6):1115–1126. doi:10.3233/XST-221220
- Langan RC, Goodbred AJ. Pulmonary nodules: common questions and answers. *Am Fam Physician*. 2023;107(3):282–291.
- Gaeta M, Barone M, Caruso R, et al. CT-pathologic correlation in nodular bronchioloalveolar carcinoma. *J Comput Assist Tomogr*. 1994;18. doi:10.1097/00004728-199403000-00011
- Akhan O, Demirkazik FB, Özmen MN, et al. Tuberculous pleural effusions: ultrasonic diagnosis. *Clin Ultrasound*. 1992;20(7):461–465. doi:10.1002/jcu.1870200708
- Ebara K, Takashima S, Jiang B, et al. Pleural invasion by peripheral lung cancer: prediction with three-dimensional CT. *Acad Radiol*. 2015;22(3):310–319. doi:10.1016/j.acra.2014.10.002
- Meisinger QC, Klein JS, Butnor KJ, Gentchos G, Leavitt BJ. CT features of peripheral pulmonary carcinoid tumors. *AJR Am J Roentgenol*. 2011;197(5):1073–1080. doi:10.2214/AJR.10.5954
- Li Q, Fan X, Huo JW, Luo TY, Huang XT, Gong JW. Differential diagnosis of localized pneumonic-type lung adenocarcinoma and pulmonary inflammatory lesion. *Insights Into Imaging*. 2022;13(1):49. doi:10.1186/s13244-022-01200-z
- Chu ZG, Sheng B, Liu MQ, Lv FJ, Li Q, Ouyang Y. Differential diagnosis of solitary pulmonary inflammatory lesions and peripheral lung cancers with contrast-enhanced computed tomography. *Clinics*. 2016;71(10):555–561. doi:10.6061/clinics/2016(10)01
- Fu BJ, Lv ZM, Lv FJ, Li WJ, Lin RY, Chu ZG. Sensitivity and specificity of computed tomography hypodense sign when differentiating pulmonary inflammatory and malignant mass-like lesions. *Quant Imaging Med Surg*. 2022;12(9):4435–4447. doi:10.21037/qims-21-851
- Zhang T, Yuan M, Zhong Y, et al. Differentiation of focal organising pneumonia and peripheral adenocarcinoma in solid lung lesions using thin-section CT-based radiomics. *Clin Radiol*. 2019;74(1):78.e23–78.e30. doi:10.1016/j.crad.2018.08.014
- Qiu Q, Xing L, Wang Y, Feng A, Wen Q. Development and validation of a radiomics nomogram using computed tomography for differentiating immune checkpoint inhibitor-related pneumonitis from radiation pneumonitis in patients with non-small cell lung cancer. *Front Immunol*. 2022;13:870842. doi:10.3389/fimmu.2022.870842
- Jiang J, Lv FJ, Tao Y, et al. Differentiation of pulmonary solid nodules attached to the pleura detected by thin-section CT. *Insights Imaging*. 2023;14(1):146. doi:10.1186/s13244-023-01504-8

27. Zwirewich CV, Vedal S, Miller RR, Muller NL. Solitary pulmonary nodule: high-resolution CT and radiologic-pathologic correlation. *Radiology*. 1991;179(2):469–476. doi:10.1148/radiology.179.2.2014294
28. Agrons GA, Courtney SE, Stocker JT, Markowitz RI. From the archives of the AFIP: lung disease in premature neonates: radiologic-pathologic correlation. *Radiographics*. 2005;25(4):1047–1073. doi:10.1148/rg.254055019
29. Mordant P, Arame A, Legras A, Le Pimpec Barthes F, Riquet M. Pleural lymphatics and effusions. *Rev Pneumol Clin*. 2013;69(3):175–180. doi:10.1016/j.pneumo.2013.01.006
30. Kim HJ, Cho JY, Lee YJ, et al. Clinical significance of pleural attachment and indentation of subsolid nodule lung cancer. *Cancer Res Treat*. 2019;51(4):1540–1548. doi:10.4143/crt.2019.057
31. Tindle HA, Stevenson Duncan M, Greevy RA, et al. Lifetime smoking history and risk of lung cancer: results from the Framingham Heart Study. *J Natl Cancer Inst*. 2018;110(11):1201–1207. doi:10.1093/jnci/djy041
32. Jiang B, Han D, van der Aalst CM, et al. Lung cancer volume doubling time by computed tomography: a systematic review and meta-analysis. *Eur J Cancer*. 2024;212:114339. doi:10.1016/j.ejca.2024.114339
33. Zwirewich CV, Miller RR, Muller NL. Multicentric adenocarcinoma of the lung: CT-pathologic correlation. *Radiology*. 1990;176(1):185–190. doi:10.1148/radiology.176.1.2162069

Journal of Inflammation Research

Publish your work in this journal

The Journal of Inflammation Research is an international, peer-reviewed open-access journal that welcomes laboratory and clinical findings on the molecular basis, cell biology and pharmacology of inflammation including original research, reviews, symposium reports, hypothesis formation and commentaries on: acute/chronic inflammation; mediators of inflammation; cellular processes; molecular mechanisms; pharmacology and novel anti-inflammatory drugs; clinical conditions involving inflammation. The manuscript management system is completely online and includes a very quick and fair peer-review system. Visit <http://www.dovepress.com/testimonials.php> to read real quotes from published authors.

Submit your manuscript here: <https://www.dovepress.com/journal-of-inflammation-research-journal>

Dovepress
Taylor & Francis Group